Available online at www.sciencedirect.com
ScienceDirect
Journal of Molecular Catalysis A: Chemical 285 (2008) 58–67
JOURNAL OF MOLECULAR CATALYSIS A: CHEMICAL
www.elsevier.com/locate/molcata

# Ship-in-a-bottle synthesis, characterization and catalytic oxidation of cyclohexane by Host (nanopores of zeolite-Y)/guest (Mn(II), Co(II), Ni(II) and Cu(II) complexes of bis(salicyaldehyde)oxaloyldihydrazone) nanocomposite materials

Masoud Salavati-Niasari [a,b,*], Azam Sobhani [b]

[a] *Institute of Nano Science and Nano Technology, University of Kashan, Kashan, P.O. Box 87317–51167, IR, Iran*
[b] *Department of Chemistry, Faculty of Science, University of Kashan, Kashan, P.O. Box 87317–51167, IR, Iran*

Received 23 October 2007; received in revised form 26 December 2007; accepted 10 January 2008
Available online 31 January 2008

**Abstract**

The monomer transition metal complexes; [ML] (M = Mn(II), Co(II), Ni(II) and Cu(II)) have been synthesized from the reaction of metal acetate with bis(salicyaldehyde)oxaloyldihydrazone, $H_2L$; in 1:1 molar ratio in ethanol under reflux. In all of the complexes, the principal dihydrazone ligand has been suggested to coordinate to the metal centres in the anti-*cis*-configuration. The complexes (Co(II), Ni(II) and Cu(II)) are suggested to have four-coordinate square-planar stereochemistry while the Mn(II) complex is suggested to have tetrahedral stereochemistry. These metal complexes with tetradendate Schiff-base ligand was entrapped in the nanocavity of zeolite-Y by a two-step process in the liquid phase: (i) adsorption of [bis(salicylaldiminato)metal(II)]; [$M(sal)_2$]-NaY; in the supercages of the zeolite, and (ii) in situ Schiff condensation of the metal(II) precursor complex with oxaloyldihydrazone; [ML]-NaY. The new Host–Guest Nanocomposite Materials (HGNM) was characterized by several techniques: chemical analysis, spectroscopic methods (DRS, NMR, BET, FTIR and UV/vis), conductometric and magnetic measurements. The catalytic activities for oxidation of cyclohexane with HGNM and neat were reported.


*Keywords:* Nanocomposite material; Host–Guest; Zeolite; Oxidation of cyclohexane

## 1. Introduction

Nanotechnology refers to techniques that offer the ability to design, synthesize, and control materials at scales ranging from <1 to >100 nm. The emphasis in this definition of scope is "design and control", and not only synthesis. Synthesis of materials at nanometer scale has already become routine practice for supported metal catalysts after decades of research on the subject. Nanotechnology has gained substantial popularity recently due to the rapidly developing techniques both to synthesize and characterize materials and devices at the nanoscale, as well as the promises that such technology offers to substantially expand the achievable limits in many different fields including medicine, electronic, chemistry, and engineering. In the literature, there are many reports of new researches about interesting phenomena of nano materials and their applications. Nanosize metal particles had occupied a central place in heterogeneous catalysis for many years long before their recognition in nanotechnology. Thus, it is fitting to critically evaluate the impact of such development on heterogeneous catalysis [1,2].

The finding of efficient catalysts for the selective insertion of one oxygen atom from oxygen donors, like PhIO, $O_2$, $H_2O_2$, *t*-BuOOH, or NaOCl into various organic molecules, under mild conditions, remains a difficult challenge in the fields of chemical and biological catalysis [3]. The oxidation of hydrocarbons by transition metal complexes has been studied extensively [4–10]. Among the inorganic mimics of enzymes, metal complexes containing porphyrin, macrocycle salen, and phthalocyanine ligands have been investigated as possible alternative catalysts in many oxidation and hydroxylation reactions [11–15]. Generally, the

* Corresponding author at: Institute of Nano Science and Nano Technology, University of Kashan, Kashan, P.O. Box 87317–51167, IR, Iran.
Tel.: +98 361 5555 333; fax: +98 361 555 29 30.
*E-mail address:* salavati@kashanu.ac.ir (M. Salavati-Niasari).

1381-1169/$ – see front matter © 2008 Elsevier B.V. All rights reserved.
doi:10.1016/j.molcata.2008.01.030

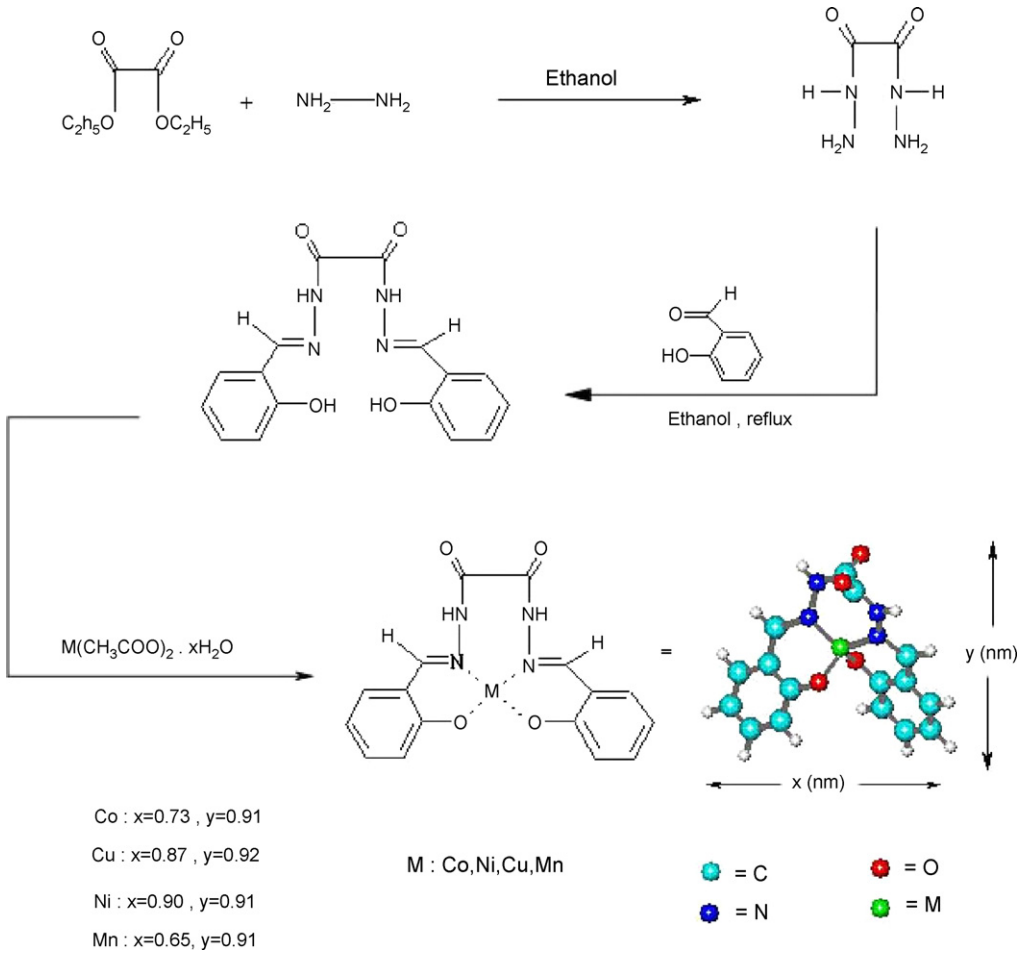


Schemes 1.

electronic and structural properties of the ligands play an important role in the catalytic properties [16–18].

The catalytic activity of the complexes in homogeneous medium decreases with time due to ligand oxidation or formation of dimeric oxo- and peroxobridged complexes. Heterogenization of the homogeneous catalysts (metal complexes) has been sought to isolate the metal complexes to prevent their isomerization, increase their ruggedness and separability and to benefit from the synergistic catalytically beneficial interaction between the complexes and the support [19–29]. Heterogenization is achieved either by encapsulating the metal complex inside the nanopores of zeolites or by anchoring or tethering them to inert supports [21–24]. Grafting and tethering refer to covalent attachment of the metal complex, either directly (grafting) or through a spacer ligand (tethering). The encapsulation (ship-in-a-bottle) approach is convenient and ideal because the complex, once formed inside the nanocages of zeolite, is too large to diffuse out and is not lost into the liquid phase during the reaction. As these composite materials mimic biological enzymes, they are also called "zeozymes" (acronym for zeolite mimics of enzymes). On confinement in the zeolite matrix, the metal complex may lose some of its degrees of freedom and adopt unusual geometries that are stabilized by coordination to the zeolite-surface functional groups. In a general sense, the encapsulated complexes mimic enzyme systems in that the porous inorganic mantle (similar to the protein mantle in enzymes) provides (hopefully) the right steric requirement for the metal complex and imposes certain requirements (based on size and shape) to the access of the active site by the substrate molecules (substrate selectivity). Though many porous materials have been used, the most popular ones have been zeolites Y possessing large nanocages (1.2 nm diameters).

In this work, we report the encapsulation of transition metal complexes in the supercages of a NaY zeolite, using the same sequential procedure: (i) diffusion of $[M(sal)_2]$, and (ii) in situ Schiff condensation with the oxaloyldihydrazone (Schemes 1 and 2). The use of a zeolite with the FAU topology, such as NaY zeolite, may circumvent hydrolysis of the occluded complexes. We will also address the effect on the structural and electronic properties of the encapsulated complexes within a host with (i) a negative charge which can hence act as a stronger ligand, and (ii) a larger number of charge-compensating cations thus providing less free space within the zeolite nanocavities (Schemes 1 and 2).

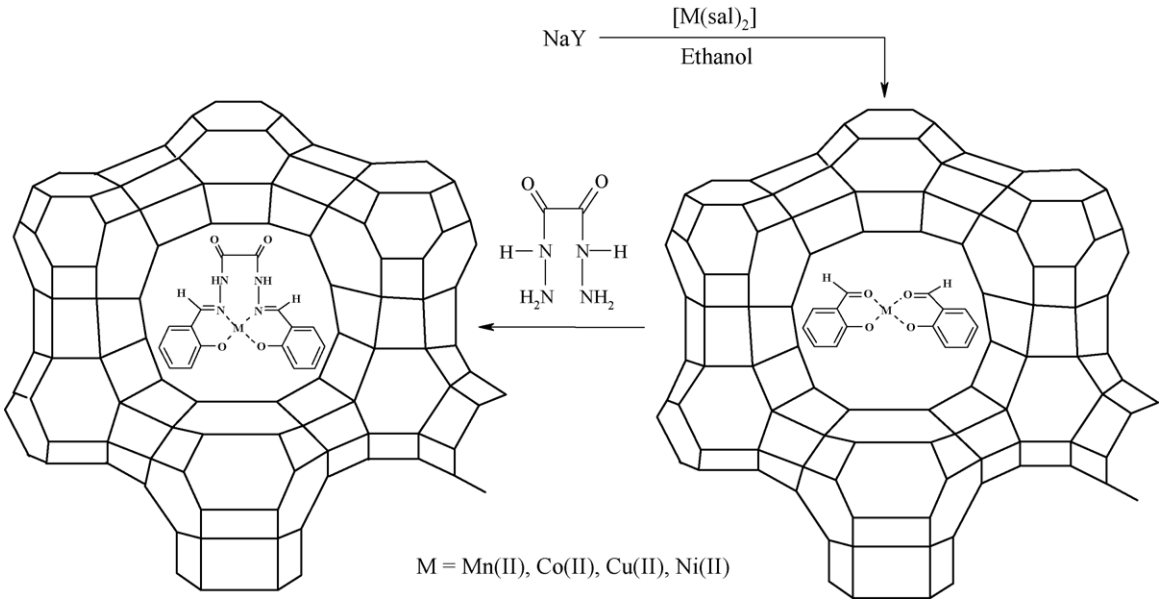


Schemes 2.

## 2. Experimental

### 2.1. Materials

All the solvents were purchased from Merck (pro analysi) and were distilled and dried using molecular sieves (Linda 4 Å). Manganese(II), copper(II), nickel(II) and cobalt(II) acetate, salicylaldehyde, diethyl oxalate, hydrazine hydrate and hydrogen peroxide were obtained from Merck Co. Cyclohexane was distilled under nitrogen and stored over molecular sieves (4 Å). Reference samples of cyclohexanol and cyclohexanone were distilled and stored in the refrigerator. NaY with the Si:Al ratio of 2.53 was purchased from Aldrich (Lot No. 67812). Oxaloyldihydrazine was prepared by reacting ethyloxalate (1 mol) with hydrazine hydrate (2 mol) [24].

### 2.2. Physical measurements

Nitrogen adsorption measurements were performed at 77 K using a Coulter Omnisorb 100CX instrument. Nanopore volumes were determined by the *t*-method; a "monolayer equivalent area" was calculated from the micropore volume [30,31]. XRD patterns were recorded by a Rigaku D-max C III, X-ray diffractometer using Ni-filtered Cu Kα radiation. Elemental analysis were obtained from Carlo ERBA Model EA 1108 analyzer. The metal contents of the samples were measured by Atomic Absorption Spectrophotometer (AAS-PerkinElmer 4100–1319) using a flame approach. After completely destroying the zeolitic framework with hot and concentrated HCl, sodium, aluminum and transition metal were analyzed by AAS and $SiO_2$ was determined by gravimetric analysis. The products were analyzed by GC–MS on a Philips Pu 4400 gas chromatograph mass spectrometer. Diffuse reflectance spectra (DRS) were registered on a Shimadzu UV/3101 PC spectrophotometer the range 1500–200 nm, using MgO as reference. The electronic spectra of the neat complexes were taken on a Shimadzu UV–vis scanning spectrometer (Model 2101 PC). The stability of the encapsulated catalyst was checked after the reaction by UV–vis and possible leaching of the complex was investigated by UV–vis in the reaction solution after filtration of the zeolite. The amounts of metallocomplexes encapsulated in zeolite matrix were determined by the elemental analysis and by subtracting the amount of metallocomplex left in the solutions after the synthesis of the catalysts as determined by UV–vis spectroscopy, from the amount taken for the synthesis. Magnetic moments were calculated from magnetic susceptibility data obtained using a Johnson Matthey MK-1 magnetic susceptibility balance and conductance measurements with a Metrohm Herisau conductometer E 518. H NMR (400 MHz) spectra were measured in DMSO solutions and referenced to the solvent signals.

### 2.3. Preparation of *Bis(salicylaldehyde)oxaloyldihydrazone*

Bis(salicylaldehyde)oxaloyldihydrazone was prepared by refluxing hot dilute ethanol solution of oxaloyldihydrazone (1 mol) with salicylaldehyde (2 mol) by the literature method [25]. The yellow precipitate obtained was crystallized from ethanol, dried in an electric oven at ca. 70 °C, m.p. >300 °C (dec).

### 2.4. Preparation of [ML] (M=Mn(II), Co(II), Ni(II), Cu(II))

The flask containing a stirred suspension of transition metal(II) acetate tetrahydrate (0.016 mol) in 100 ml ethanol (was purged with nitrogen) and then warmed to 50 °C under a nitrogen atmosphere. Bis(salicylaldehyde)oxaloyldihydrazone; $H_2L$; (5.22 g, 0.016 mol) and $Et_3N$ (4.46 ml, 0.032 mmol) were added in one portion, and the resulting suspension was then stirred and heated under nitrogen atmosphere for 8 h. Then the mixture was

cooled and filtered under reduced pressure. The collected solid was washed with diethylether and dried in air to give coloured crystalline, [ML], which was purified by recrystallization from dimethylformamid.

### 2.5. Preparation of [M(sal)$_2$]-NaY

Typically a 4 g sample of NaY zeolite was mixed with 0.36 g of [bis(salicylaldiminato)metal(II)] (which corresponds to about 50% supercage loading), suspended in 40 ml of $CHCl_3$ and then refluxed for 8 h. The coloured solid consisting of [M(sal)$_2$] entrapped in NaY and denoted as [M(sal)$_2$]-NaY was collected by filtration, washed with cold ethanol (10 ml) and then dried at 90 °C under vacuum for 5 h.

### 2.6. Preparation of [ML]-NaY

Two grams of [M(sal)$_2$]-NaY was refluxed with a threefold excess of oxaloyldihydrazone in $CH_3OH$. After a 3 h reflux, the solid samples, [ML]-NaY, were filtered and the resulting zeolites were Soxhlet extracted with *N*,*N*-dimethylformamide (for 4 h) and then with ethanol (for 3 h) to remove excess oxaloyldihydrazone, unreacted [M(sal)$_2$] and any M(II) complexes adsorbed onto the external surface of the zeolite crystallites. The resulting solids were dried at 90 °C under vacuum for 10 h.

### 2.7. Oxidation of cyclohexane

Aqueous solution of 30% $H_2O_2$ (2.28 g, 20 mmol), cyclohexane (0.84 g, 10 mmol) and catalyst ($1.02 \times 10^{-5}$ mol) were mixed in 5 ml of $CH_3CN$ and the reaction mixture was heated at 70 °C with continuous stirring in an oil bath for 2 h. After filtering and washing with solvent, the filtrate was concentrated and then subjected to GC analysis.

## 3. Results and discussion

### 3.1. Synthesis of complexes

The analytical data and physical properties of the ligands and coordination compounds are listed in Table 1. The results from Table 1 show that the ligands coordinate to the metal ion in a 1:1 molar ratio. The ligand is soluble in hot ethanol and strong polar solvents such as in DMF and DMSO. All of the compounds are stable in air. The melting points of the complexes are higher than the ligand revealing that the complexes are much more stable than the ligand. These complexes have molar conductance values in the region 11–19 $ohm^{-1}\,cm^2\,mol^{-1}$ in DMSO indicating that they are non-electrolyte in this solvent [32]. The molar conductance values for these complexes lie in the non-electrolytic region which rules out the possibility of their ionic character. In view of the non-ionic nature of these complexes and proximity of the experimental molecular weights with the theoretical values for the monomer formulation, these complexes are also suggested to be monomer.

Table 1
Elemental analysis, vibrations parameters and some physical properties for Schiff-base neat metal(II) complexes

| Complex | Elemental analysis calcd. (found)% | | | | | $\Lambda_M$[a], $\Omega^{-1}\,cm^2\,M^{-1}$ | $\mu_{eff}$ (MB) | IR (KBr, $cm^{-1}$) | | | | | d ↔ d (nm)[b] |
|---|---|---|---|---|---|---|---|---|---|---|---|---|---|
| | %C | %H | %N | C/N | %M | | | ν(C=O) | ν(N–N) | ν(C=N) | ν(M–$O_{phenolic}$) | ν(N–H) | amide(II) + ν($CO_{phenolic}$) | |
| $H_2L$ | 58.88 (58.65) | 4.32 (4.20) | 17.17 (17.30) | 3.43 (3.39) | – | – | – | 1688 (vs) | 1035 (w) | 1625 (s) | – | 3210 (s) | 1530 (m) | 330, 370 |
| [MnL] | 50.67 (50.44) | 3.19 (3.04) | 14.77 (14.86) | 3.43 (3.39) | 14.49 (14.33) | 11 | 5.92 | 1693 (vs) | 1036 (w) | 1620 (s) | 530 (w) | 3206 (s) | 1538 (m) | – |
| [CoL] | 50.15 (49.91) | 3.16 (2.97) | 14.62 (14.78) | 3.43 (3.38) | 15.38 (15.20) | 14 | 1.72 | 1695 (vs) | 1036 (w) | 1619 (s) | 530 (w) | 3207 (s) | 1540 (m) | 570, 630 |
| [NiL] | 50.18 (50.01) | 3.16 (3.01) | 14.63 (14.80) | 3.43 (3.38) | 15.32 (15.12) | 16 | Dia. | 1696 (vs) | 1035 (w) | 1620 (s) | 531 (w) | 3204 (s) | 1537 (m) | 475 |
| [CuL] | 49.55 (49.33) | 3.12 (3.02) | 14.45 (14.59) | 3.43 (3.38) | 16.38 (16.22) | 19 | 1.73 | 1699 (vs) | 1036 (w) | 1617 (s) | 532 (w) | 3202 (s) | 1538 (m) | 487, 556 |

[a] In DMSO solution.
[b] In chloroform solutions.

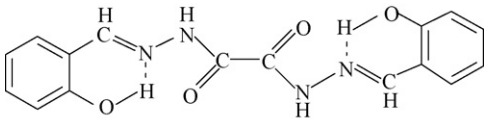

Staggered-configuration

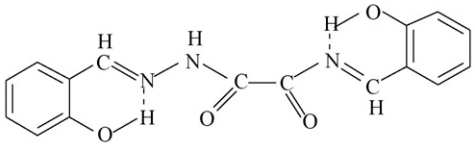

Syn-cis-configuration

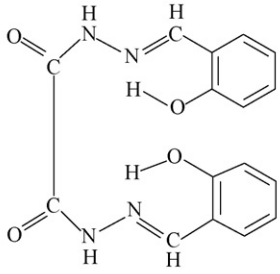

Anti-cis-configuration

Schemes 3.

### 3.2. $^1H$ NMR spectra

The $^1H$ NMR spectrum of $H_2L$ has been recorded in DMSO-$d_6$ as it is insoluble in $CHCl_3$. The $^1H$ NMR spectra of the ligand and the nickel(II) complexes have been studied. The four and two proton signals observed at $\delta$ 12.38 ppm and $\delta$ 8.60 ppm downfield of TMS have been assigned to the $\delta$ OH + $\delta$ NH and $\delta$ CH=N protons, respectively. The multiplet appearing in the region $\delta$ 6.61–7.40 ppm has been assigned to phenyl protons. Because of their diamagnetic character, the nickel(II) complex has been studied by $^1H$ NMR spectroscopy. The nickel(II) complex shows two signals at $\delta$ 12.31 and 8.71 ppm. The feature of these signals suggests that they arise due to NH protons. The $\delta$ CH=N signal observed at $\delta$ 8.60 ppm also splits into two resonances and appears in the region $\delta$ 8.71 ppm. This signal shows downfield shift of about 0.11 ppm. The splitting of this signal into two signals shows the effect of coordination of dihydrazone through the azomethine nitrogen atoms to the metal centre. The splitting of $\delta$ NH and CH=N signals indicates that the conformation of dihydrazone is changed from staggered to anti-*cis* conformation in the complexes (Scheme 3) [33].

### 3.3. Magnetic moment

The $\mu_B$ value for [NiL] complex is zero indicating that this is diamagnetic. It is clear that $Ni^{+2}$ is $d^8$ low spin electronic configuration. Copper(II) complex shows $\mu_B$ values in the 1.73 BM. This value is close to the spin-only value. This magnetic moment range indicates the absence of any appreciable spin–spin coupling between unpaired electrons belonging to different molecules. According to Figgis [34], a magnetic moment value greater than 1.90 BM indicates tetrahedral stereochemistry, while a $\mu_B$ value less than 1.90 BM is indicative of square-planar as well as tetrahedral stereochemistry. This shows that the magnetic susceptibility is not of much use in deciding on the stereochemistry of copper(II) complexes. On the other hand, the compounds [MnL] and [CoL] are paramagnetic to the extent of 5.92 and 1.72 BM, respectively (Table 1). The $\mu_B$ values for the complexes are close to the spin-only value for a formally $d^5$ high spin (for [MnL]) and $d^7$ low spin (for [CoL]) system. This feature can be interpreted as being indicative of the effective quenching of the orbital angular momentum by a low symmetry ligand field surrounding the metal centre. The $\mu_B$ values in the present M(II) complexes dismiss the possibility of any significant metal–metal interactions.

### 3.4. Ship-in-a-bottle encapsulation

Ship-in-a-bottle encapsulation of the complexes was performed in the liquid phase by a two-step process that involves (i) adsorption of a transition metal precursor complex, [M(sal)$_2$]-NaY (M=Mn(II), Co(II), Ni(II), Cu(II)), and (ii) in situ Schiff condensation of the adsorbed metal complex with the oxaloyldihydrazone; [ML]-NaY. The resulting materials, [ML]-NaY, were purified by Soxhlet extraction with diffent solvents. In order to characterise the resulting materials and to assess the efficiency of the encapsulation process, the parent zeolite and samples of [M(sal)$_2$]-NaY and [ML]-NaY, were studied by several techniques and the obtained results compared. Soxhlet extraction was performed only for the zeolites with the complexes [ML]; the modified zeolites with [M(sal)$_2$] were not purified by extraction as it was observed that this operation leads to a loss of the characteristic colour of the material. This observation provides an indication that [M(sal)$_2$] is free to diffuse out of the zeolite. As these samples were not submitted to Soxhlet extraction, it was expected that they have metal complexes both inside the nanocavities and adsorbed onto the external surface. The chemical compositions confirmed the purity and stoichiometry of the neat and nanocavity encapsulated complexes (Tables 1 and 2). The chemical analysis of the samples reveals the presence of organic matter with a C/N ratio roughly similar to that for neat complexes. The mol ratios Si/Al obtained by chemical analysis for zeolites are presented (Table 2). The Si and Al contents in M(II)-NaY and the zeolite complexes; [ML]-NaY; are almost in the same ratio as in the parent zeolite. This indicates little changes in the zeolite framework due to the absence of dealumination in metal ion exchange.

The in situe Schiff condensation synthesis, Scheme 2, leads to the encapsulation of manganese(II), cobalt(II), nickel(II) and copper(II) complexes of bis(salicylaldehyde)oxaloyldihydrazone ligand within the nanodimensional pores of zeolite. The parent NaY zeolite has Si/Al molar ratio of 2.53 which corresponds to a unit cell formula $Na_{56}[(AlO_2)_{56}(SiO_2)_{136}]$ (Table 2). The unit cell formulae of metal-exchanged zeolites show a metal dispersion of around 11 mol per unit cell (Mn(II)-NaY, $Na_{33.2}Mn_{11.3}[(AlO_2)_{56}(SiO_2)_{136}]\cdot nH_2O$; Co(II)-NaY, $Na_{34}Co_{11}[(AlO_2)_{56}(SiO_2)_{136}].nH_2O$; Ni(II)-

Table 2
Chemical composition, DRS absorption and IR stretching frequencies (as KBr pellets) of zeolite-encapsulated metal(II) complexes

| Sample | C (%) | H (%) | N (%) | C/N | Si (%) | Al (%) | Na (%) | M (%) | Si/Al | $\nu_{C=N}$ ($cm^{-1}$) | d ↔ d (nm) |
|---|---|---|---|---|---|---|---|---|---|---|---|
| NaY | – | – | – | – | 21.76 | 8.60 | 7.50 | – | 2.53 | – | – |
| Mn(II)-NaY | – | – | – | – | 22.08 | 8.73 | 3.34 | 2.58 | 2.53 | – | – |
| [MnL]-NaY | 3.06 | 1.21 | 0.96 | 3.19 | 21.56 | 8.52 | 5.33 | 2.31 | 2.53 | 1620 | – |
| Co(II)-NaY | – | – | – | – | 21.53 | 8.53 | 3.36 | 3.71 | 2.53 | – | – |
| [CoL]-NaY | 3.08 | 1.19 | 0.95 | 3.24 | 21.54 | 8.51 | 5.30 | 2.29 | 2.53 | 1617 | 568 |
| Ni(II)-NaY | – | – | – | – | 21.79 | 8.62 | 3.28 | 3.72 | 2.53 | – | – |
| [NiL]-NaY | 2.95 | 1.18 | 0.93 | 3.17 | 21.48 | 8.49 | 5.26 | 2.28 | 2.53 | 1610 | 474 |
| Cu(II)-NaY | – | – | – | – | 21.48 | 8.49 | 3.28 | 3.86 | 2.53 | – | – |
| [CuL]-NaY | 2.90 | 1.16 | 0.90 | 3.22 | 21.57 | 8.52 | 5.28 | 2.26 | 2.53 | 1606 | 553 |

NaY, $Na_{33.8}Ni_{11.1}[(AlO_2)_{56}(SiO_2)_{136}]\cdot nH_2O$; Cu(II)-NaY, $Na_{34.4}Cu_{10.8}[(AlO_2)_{56}(SiO_2)_{136}]\cdot nH_2O$). The analytical data of each complex indicate M:C:H molar ratios almost close to those calculated for the mononuclear structure.

### 3.5. IR spectral study

The uncoordinated ligand shows strong bands at 1688 and 1625 $cm^{-1}$ which are assigned to stretching vibrations of C=O and C=N group. These bands split into two bands and on average, undergo shift to higher position by 5–11 $cm^{-1}$ and lower position by 5–8 $cm^{-1}$, respectively. The average shift of $\nu$C=O band to higher frequency by ca. 5–11 $cm^{-1}$ and of $\nu$C=N band to lower frequency by 8–11 $cm^{-1}$ in complexes suggests non-coordination of C=O group while coordination of dihydrazone through C=N groups, to the metal centre. The band at 1530 $cm^{-1}$ assigned to amide II + $\nu$(C=O) (phenolic) shifts to higher frequency ruling out the possibility of coordination of ligand to the metal centre through CO groups. This further indicates involvement of phenolate oxygen atom in bonding to the metal centre. The shift of band at 1278 $cm^{-1}$ to higher frequency by ~5 $cm^{-1}$ and appearance of medium to strong bands at 530 $cm^{-1}$ confirms the coordination of dihydrazone to the metal centre through Scheme 1.

FTIR data can provide information on the encapsulated metal complexes and on the crystallinity of the host zeolite. The FTIR spectra of NaY and of the modified zeolites are studied (Fig. 1). The spectra of NaY and of the modified zeolites are dominated by the strong zeolite bands: a broad band in the range 3700–3300 $cm^{-1}$ due to surface hydroxylic groups and lattice vibrations in the range 1300–450 $cm^{-1}$. No shift or broadening of these zeolite structure-sensitive vibrations are observed upon inclusion of the complexes, which provides further evidence that the zeolite framework remains unchanged. The bands due to the complexes are weaker (due to a low concentration of the complexes) and thus can only be observed in the regions where the zeolite matrix does not absorb, i.e. from 1620 to 1200 $cm^{-1}$. The IR bands of [ML]-NaY occur at frequencies shifted within 2–4 $cm^{-1}$ from those of the free complex [ML]; furthermore, some changes in band intensities can be observed in the region of the C=O and C=C stretching vibrations (1520–1580 $cm^{-1}$). These observations not only confirm the presence of [ML] in the zeolite, but also suggest that its structure is almost identical to that of the free complex. The IR spectra of [ML] clearly show the absence of the characteristically coupled $\nu$(C=O) + $\nu$(C=C) vibration of [ML], as expected from the Schiff condensation that took place within the zeolite cavities. The entrapped complexes exhibit very similar IR data that are shifted 4–8 $cm^{-1}$ relative to those of the corresponding free complexes (Table 2). These variations in band frequency can also be attributed to (i) distortions of the complexes, or to (ii) interactions with the zeolitic matrix (by electrostatic effects or co-ordination- the higher negative charge of the zeolite host makes it a stronger ligand).

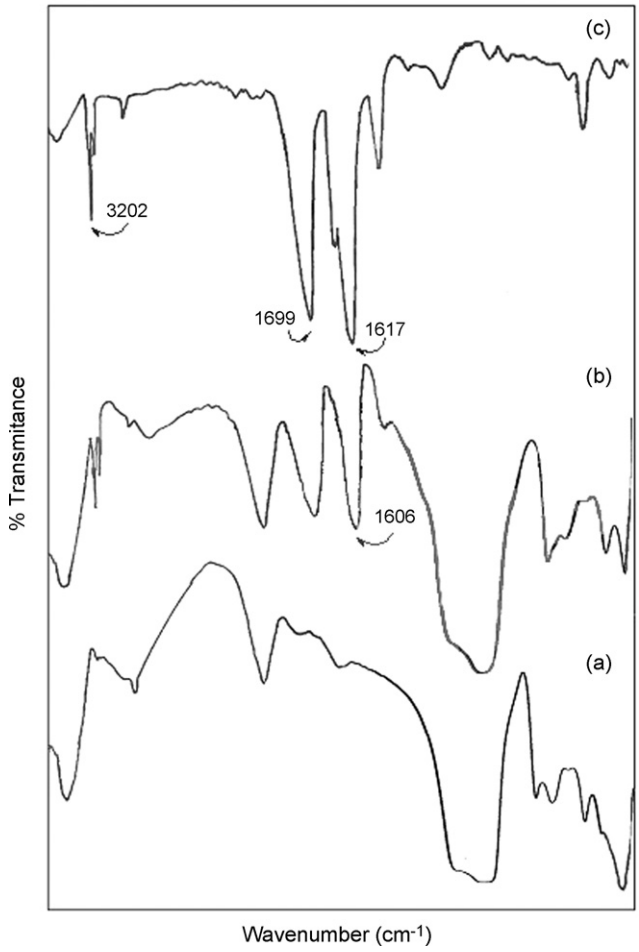


Fig. 1. FT-IR spectra of: (a) NaY, (b) [CuL]-NaY and (c) [CuL].

### 3.6. Electronic spectral studies

The electronic spectrum of $H_2L$ shows bands at 330 and 370 nm in the solid state which arise due to $\pi \rightarrow \pi^*$ and $n \rightarrow \pi^*$ transitions in dihydrazone. Electronic spectra of [CuL] complexes were recorded in DMF solution over the range 400–700 nm (Table 1). The visible spectra of the [CuL] complexes consists of a shoulders at ~487 nm and a maximum or a broad shoulder around 556 nm, which can be assigned to the $dxz,yz \rightarrow dxy$ and $dx^2-y^2 \rightarrow dxy$ transitions in $D_2h$ symmetry [35]. The room temperature magnetic moments of [CuL] (Table 1) fall in the range 1.73 $\mu_B$ which are typical for square-planar ($D_4h$) and tetrahedrally distorted ($D_2h$) mononuclear copper(II) complexes with a $S = 1/2$ spin state and did not indicate any anti-ferromagnetic coupling of spines at this temperature. The tetrahedral geometry of the [MnL] is strongly indicated by similarities in the visible spectra of this chelate with those of known tetrahedral complexes containing oxygen–nitrogen donor atoms [36]. The electronic spectrum of the [NiL] exhibit one band at 475 nm which can be assigned to a d↔d transition of the metal ion. The average energy of this absorption is comparable to d↔d transitions of other square-planar Schiff-base of nickel(II) chelates with nitrogen and oxygen donor atoms [37], which have reported values in the range of 460–490 nm. The electronic spectrum of [CoL] is very similar to that reported for [Co(salen)]. The spectrum of the [CoL] exhibits two bands at 570 and 630 nm which are assigned to d↔d transitions. In addition, a lower energy absorption at 425 nm has been observed such low energy bands which have recently been shown to be characteristic of square-planar cobalt(II) chelates [38]. This geometry is confirmed by the values of the effective magnetic moment (Table 1).

### 3.7. X-ray diffraction, surface area and micropore volume study

The X-ray diffraction (XRD) patterns of zeolite contained bis(salicylaldehyde)oxaloyldihydrazone; $H_2L$; complexes are similar to those of M(II)-NaY and the parent NaY zeolite. The zeolite crystallinity is retained on encapsulating complexes. Crystalline phase of free metal ions or encapsulation ligand complexes were not detected in any of the patterns as their fine dispersion in zeolite might have rendered them non-detectable by XRD. The surface area and micropore volume of the catalysts used in the oxidation reaction are presented in Table 3. The encapsulation of metal complex reduced the surface area and adsorption capacity of zeolite. The lowering of the pore volume and surface area supported the fact that [ML]-NaY complexes are present within the zeolite nanocages and not on the external surface.

### 3.8. Catalytic activity

The major products of oxidation of cyclohexane are cyclohexanone and cyclohexanol. The zeolite-encapsulated complexes did not undergo any colour change during the reaction and could be easily separated and reused many times. In contrast, the neat complexes, while they were active in the first cycle, were completely destroyed during the first run and changed colour (Table 4). The bis(salicyaldehyde)oxaloyldihydrazone ligand alone in the absence of metal were not catalytically active. At the end of reaction, the catalyst was separated by filtrations, thoroughly washed with solvent and reused under similar conditions by AAS which showed no reduction in the amount of metal.

Table 3
Surface area and pore volume data of bis(salicyaldehyde)oxaloyldihydrazone metal(II) complexes encapsulated in nanopores of zeolite Y

| Sample | Surface area ($m^2$/g)[a] | Pore volume (ml/g) [b] |
|---|---|---|
| NaY | 545 | 0.31 |
| Mn(II)-NaY | 535 | 0.30 |
| [MnL]-NaY | 390 | 0.19 |
| Co(II)-NaY | 532 | 0.30 |
| [CoL]-NaY | 378 | 0.20 |
| Ni(II)-NaY | 528 | 0.30 |
| [NiL]-NaY | 375 | 0.21 |
| Cu(II)-NaY | 532 | 0.30 |
| [CuL]-NaY | 373 | 0.22 |

[a] Surface area is the "monolayer equivalent area" calculated as explained in reference [29] and [30].
[b] Calculated by the *t*-method.

The trend observed in Tables 4 and 5 can be explained by the donor ability of ligand available in the complex catalysts. As Wang and our work have pointed out recently, the key point in the conversion of substrate to the products is the reduction of $L–M^{(n+1)+}$ to $L–M^{n+}$. This reduction to $L–M^{n+}$ is facilitated with the ligands available around the metal cation [39–41]. No oxidation of cyclohexane occurred in the absence of the catalyst. The transition metal salt, $M(OAc)_2 \cdot xH_2O$ did not catalyze oxidation of cyclohexane under the above conditions.

The effect of transition metal complexes encapsulated in zeolite; [ML]-NaY was studied on the oxidation of cyclohexane with hydrogen peroxide in $CH_3CN$ and the results are shown in Table 5. As shown in Table 5, oxidation has occurred with the

Table 4
Oxidation of cyclohexane with $H_2O_2$ catalyzed by bis(salicyaldehyde)oxaloyldihydrazone transition metal complexes in $CH_3CN$[a]

| Catalyst | Conversion (%) | Selectivity (%) | |
|---|---|---|---|
| | | Cyclohexanol | Cyclohexanone |
| [MnL] | 12.6 | 35.9 | 64.1 |
| [CoL] | 31.2 | 31.6 | 68.4 |
| [NiL] | 5.7 | 29.5 | 70.5 |
| [CuL] | 46.8 | 28.4 | 71.6 |
| [CuL][b] | 29.1 | 57.6 | 42.4 |
| [CuL][c] | 39.2 | 23.9 | 76.1 |
| [CuL][d] | 20.0 | 17.6 | 82.4 |

[a] Reaction condition: time, 2 h; cyclohexane, 10 mmol; catalyst, $1.02 \times 10^{-5}$ mol; $H_2O_2$, 20 mmol; $CH_3CN$, 5 ml.
[b] A similar procedure as system a was carried out with $0.5 \times 10^{-5}$ mol catalyst instead of $1.02 \times 10^{-5}$ mol.
[c] A similar procedure as system a was carried out with $2.04 \times 10^{-5}$ mol catalyst.
[d] A similar procedure as system a was carried out with $4.08 \times 10^{-5}$ mol catalyst.

Table 5
Oxidation of cyclohexane with $H_2O_2$ catalyzed by HGNM in $CH_3CN$[a]

| Catalyst | Conversion (%) | Selectivity (%) | |
|---|---|---|---|
| | | Cyclohexanol | Cyclohexanone |
| [MnL]-NaY | 8.4 | 25.9 | 74.1 |
| [CoL]-NaY | 28.6 | 22.4 | 77.6 |
| [NiL]-NaY | 2.1 | 20.3 | 79.7 |
| [CuL]-NaY | 42.9 | 17.5 | 82.5 |
| [CuL]-NaY[b] | 41.4 | 18.2 | 81.8 |
| [CuL]-NaY[c] | 40.7 | 18.8 | 81.2 |
| [CuL]-NaY[d] | 40.2 | 19.3 | 80.7 |
| [CuL]-NaY[e] | 14.7 | 42.6 | 57.4 |
| Cu(II)-NaY | 10.6 | 11.7 | 88.3 |

[a] Reaction condition: time, 2 h; cyclohexane, 10 mmol; catalyst, $1.02 \times 10^{-5}$ mol; $H_2O_2$, 20 mmol; $CH_3CN$, 5 ml.
[b] First reuse.
[c] Second reuse.
[d] Third reuse.
[e] Poisoned.

formation of cyclohexanol and cyclohexanone. Oxidation with the same oxidant in the presence of Cu(II)-NaY was 10.6%. The increase of conversion from 10.6% to 42.9% compared to Cu(II)-NaY with [CuL]-NaY indicates that the existence of ligand has increased the activity of the catalyst by a factor of 4.05. From the indicated results in Table 5 it is evident that cyclohexanone is selectively formed in the presence of all catalysts. The activity of cyclohexane oxidation decreases in the series [CuL]-NaY > [CoL]-NaY > [MnL]-NaY > [NiL]-NaY.

Under the studied reaction conditions, the catalyst showed higher activity with $CH_3CN$ solvent compared to other solvents. Solvent plays an important, and sometimes decisive role in catalytic behavior because it can make different phases uniform, thus promoting mass transportation, and could also change the reaction mechanism by affecting the intermediate species, the surface properties of catalysts and reaction pathways [39]. It was found in our experiment that $CH_3CN$ was the only solvent to exhibit good catalytic activity under the described conditions in the experimental section. In contrast, when $CH_3OH$, $C_2H_5OH$, $(CH_3)_2CO$, $CH_3Cl$ and $H_2O$ were used as solvents, no activity could be detected.

The recycle ability of encapsulated complexes; [CuL]-NaY; has been tested in catalytic oxidation of cyclohexane. In a typical experiment the reaction mixture after a contact time of 2 h was filtered and after activating the catalyst by washing with acetonitrile and drying at ca. 120 °C, it was subjected to further catalytic reaction under similar conditions. No appreciable loss in catalytic activity suggests that complex is still present in the nanocavity of the zeolite-Y. The filtrate collected after separating the used catalyst was placed into the reaction flask and the reaction was continued after adding fresh oxidant for another 2 h. The gas chromatographic analysis showed no improvement in conversion and this confirms that the reaction did not proceed upon removal of the solid catalyst. The reaction was, therefore, heterogeneous in nature. No evidence for leaching of metal or decomposition of the catalyst complex was observed during the catalysis reaction and no metal could be detected by atomic absorption spectroscopic measurement of the liquid reaction

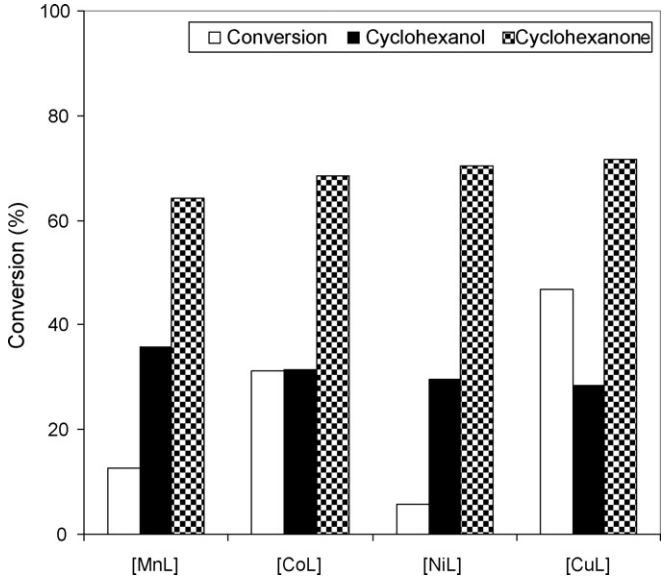


Fig. 2. Conversion and oxidation products distribution in acetonitrile with neat bis(salicyaldehyde)oxaloyldihydrazone complexes in the oxidation of cyclohexane with hydrogen peroxide (Reaction condition: time, 2 h; cyclohexane, 10 mmol; catalyst; $1.02 \times 10^{-5}$ mol).

mixture after each catalytic reaction. The IR spectrum of the solid catalyst after reuse was also identical to the fresh catalyst. Also, the catalytic behavior of the separated liquid was tested by addition of fresh cyclohexane to the filtrates after each run. Execution of the oxidation reaction under the same reaction conditions, as with catalyst, showed that the obtained results are the same as blank experiments.

The catalytic activities of encapsulated cobalt(II), manganese(II), nickel(II) and copper(II) complexes for the oxidation of cyclohexane with hydrogen peroxide in acetonitrile are represented in Table 4 and Fig. 2. Zeolite Cu(II) complexes have

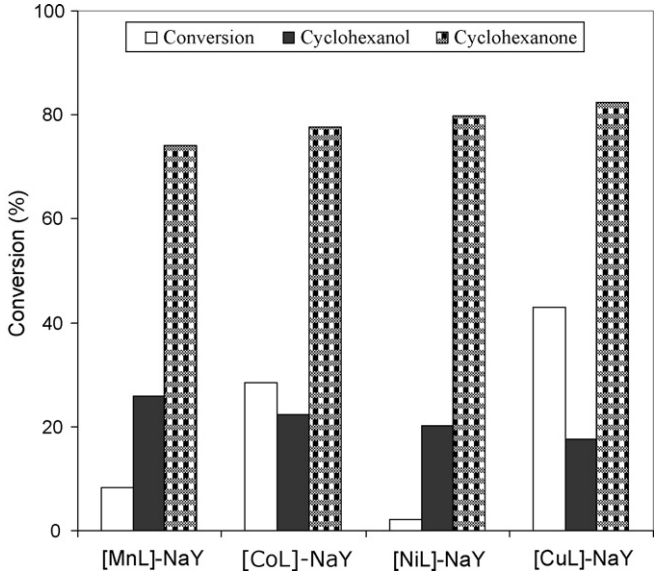


Fig. 3. Conversion and oxidation products distribution in acetonitrile with HGNM in the oxidation of cyclohexane with hydrogen peroxide (Reaction condition: time, 2 h; cyclohexane, 10 mmol; catalyst, $1.02 \times 10^{-5}$ mol).

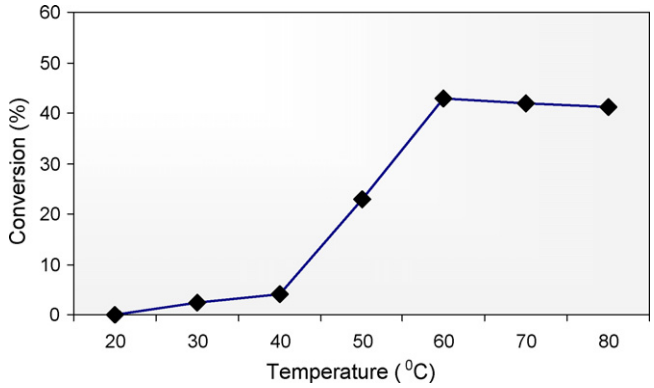


Fig. 4. Effect of temperature on substrate conversions in the oxidation of cyclohexane with $H_2O_2$ in the presence of [CuL]-NaY as catalyst (Reaction condition: time, 2 h; cyclohexane, 10 mmol; catalyst, $1.02 \times 10^{-5}$ mol).

exhibited reasonably good activity, whereas Mn(II), Ni(II) and Co(II) complexes are weakly active. Zeolite Cu(II) complexes were thoroughly evaluated for catalytic efficiency at various conditions; the results are given in Table 5 and Fig. 3. Encapsulated Cu(II) complexes are found to be active for the oxidations in the presence of $H_2O_2$ as initiator. It is interesting to note that the catalytic performances of zeolite Cu(II) complexes are comparable to the activity exhibited by the encapsulated ligand complexes reported earlier [42]. Tetrahedrally distorted square-planar geometries of zeolite Cu(II) complexes may account for their higher activity as the complexes readily provide the vacant coordination sites for oxygen binding.

Effect of reaction temperature on cyclohexane conversion is illustrated in Fig. 4. As expected, cyclohexane conversion increased with increasing reaction temperature although no conversion was detected when the reaction temperature was below 25 °C. However, high temperature led to a quick decomposition of $H_2O_2$, as a consequence, conversely lowering down the conversion. The optimum temperature was 60 °C.

Fig. 5 shows that cyclohexane conversion increased with the increase in the reaction time up to 2 h. An attempt to further increase the cyclohexane conversion by prolonging the reaction

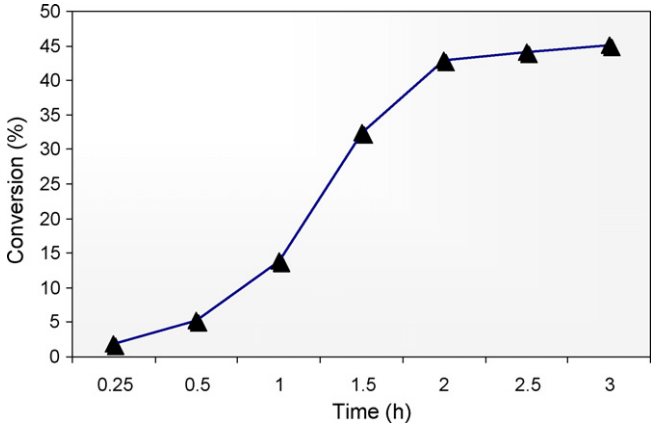


Fig. 5. Effect of time on substrate conversions in the oxidation of cyclohexane with $H_2O_2$ in the presence of [CuL]-NaY as catalyst (Reaction condition: time, 2 h; cyclohexane, 10 mmol; catalyst, $1.02 \times 10^{-5}$ mol).

time failed: about 94% of the added $H_2O_2$ was consumed when the reaction was carried out for 2 h.

Poison-tolerance of [CuL]-NaY was indirectly ascertained by evaluating their activity for the oxidation of cyclohexane in the presence of traces of pyridine which acts as a poison by coordinating irreversibly at the active site. The extent of deactivation of the catalyst, given by the loss in activity, could be related to the mobility of poison molecules at the active site. The given conversion results in Table 5 show that [CuL]-NaY has experienced a higher degree of deactivation (66% loss in conversion). It is widely believed that the stereochemical environment of the active site has a profound influence on the mobility of molecules at the reaction center and hence on the poison-tolerance.

The HGNM are believed to be stable and reusable [43–48]. In order to ascertain the stability, the catalyst samples were filtered out after the reaction, washed with acetone and analyzed by IR spectra. No changes in spectra were observed, indicating that the coordination in encapsulated complexes is retained. Furthermore, the catalyst samples could be recovered from the reaction mixture and reused without any major loss in activity (Table 5). The recycling ability also points out the absence of any irreversible deactivation of the encapsulated complexes, which is one of the major drawbacks of unsupported metal complexes in homogeneous catalytic reactions.

## 4. Conclusion

In the present study, we have prepared some monomeric transition metal complexes and characterized them on the basis of data obtained from physicochemical and spectroscopic studies. The dihydrazone coordinates to the metal centre through azomethine nitrogen atoms and phenolate oxygen atoms as a tetradentate $N_2O_2$ donor. The C=O and N–H groups remain uncoordinated. The transition metal centre has four coordinate square-planar geometry in the complexes (cobalt(II), nickel(II) and copper(II)) while it has tetrahedral coordinate geometry in the complexes (manganese(II)). In all of the complexes, the principal dihydrazone ligand is coordinated to the metal centre in keto form in the anti-*cis*-configuration. Nanopores of zeolite-encapsulated Mn(II), Co(II), Ni(II) and Cu(II) complexes of ligand and have been synthesized using the ship-in-a-bottle. Encapsulated complexes exhibit fairly clear evidence in the physico-chemical (XRD, BET) and IR spectral characterization for the well-defined inclusion and distribution of complexes in the nanopores of zeolite matrix. Tentative assignments are made for the geometry of complexes on the basis of magnetic moment, UV–vis and DRS data. Nanopores of zeolite copper(II) complexe; [CuL]-NaY; are reasonably good catalysts for the partial oxidation of cyclohexane with hydrogen peroxide, whereas Mn(II), Co(II) and Ni(II) are weakly active. The encapsulated complexes are believed to be stable and reusable due to the following reasons: (1) complexes are immobilized in the cavities, (2) reduced formation of inactive oxo and peroxo dimeric and other polymeric species in the cavities due to the steric effects of zeolite framework and (3) the interaction of encapsulated complexes with the zeolite lattice. This catalytic system showed high activity in oxidation of cyclohexane under mild reaction

conditions. Encapsulated complex, HGNM, can be recovered and reused without the loss of catalytic activity. The catalytic behavior could be mainly attributed to the geometry of encapsulated complexes. Activity and poison-tolerance of the catalysts are dependent on the mobility of molecules, which is related to the diffusion limitations due to the steric hindrance at the metal center.

## References


[1] G.A. Somorjai, Y.G. Borodko, Catal. Lett. 76 (2001) 1.
[2] H.H. Kung, M.C. Kung, Appl. Catal. A Gen. 246 (2003) 193.
[3] M. Beller, C. Bolm (Eds.), Transition Metals for Organic Synthesis, vol.2, Wiley–VCH, Weinheim, 1998.
[4] D.E. de Vos, P.P. Knops-Gerrits, D.L. Vanoppen, P.A. Jacobs, Supramol. Chem. 6 (1995) 49.
[5] P.P. Knops-Gerrits, D.E. de Vos, P.A. Jacobs, J. Mol. Catal. A 117 (1997) 57.
[6] D. Kumar, E. Derat, A.M. Khenkin, R. Neuman, S. Shaik, J. Am. Chem. Soc. 127 (2005) 17712.
[7] R.L. Cropley, F.J. Williams, A.J. Urquhart, O.P.H. Vaughan, M.S. Tikhov, R.M. Lambert, J. Am. Chem. Soc. 127 (2005) 6069.
[8] M. Salavati-Niasari, A. Amiri, J. Mol. Catal. A Chem. 235 (2005) 114.
[9] M. Salavati-Niasari, A. Amiri, Trans. Met. Chem. 31 (2006) 157.
[10] M. Salavati-Niasari, M. Bazarganipour, Inorg. Chem. Commun. 9 (2006) 332.
[11] N. Herron, Inorg. Chem. 25 (1986) 4714.
[12] R. Raja, P. Ratnasamy, Stud. Surf. Sci. Catal. 101 (1996) 187.
[13] C.R. Jacob, S.P. Varkey, P. Ratnasamy, Appl. Catal. A 168 (1998) 353.
[14] M. Salavati-Niasari, Inorg. Chem. Commun. 7 (2004) 698.
[15] M.R. Maurya, U. Kumar, P. Manikandan, Dalton Trans. (2006) 3561.
[16] M. Salavati-Niasari, Micropor. Mesopor. Mat. 92 (2006) 173.
[17] E.N. Jacobsen, W. Zhang, M. Güler, J. Am. Chem. Soc. 113 (1991) 6703.
[18] E.N. Jacobsen, in: E.W. Abel, F.G.A. Stone, G. Wilkinson, L.S. Hegedus (Eds.), Comprehensive.
[19] N. Herron, Chemtech 19 (1989) 542.
[20] P.-P. Knops-Gerrits, D.E. De Vos, F. Thibault-Starzyck, P.A. Jacobs, Nature 369 (1994) 543.
[21] K.J. Balkus Jr., A.G. Gabrielov, J. Incl. Phenom. Mol. Recog. Chem. 21 (1995) 159.
[22] M. Salavati-Niasari, J. Mol. Catal. A Chem. 245 (2006) 192.
[23] M. Salavati-Niasari, P. Salemi, F. Davar, J. Mol. Catal. A Chem. 238 (2005) 215.
[24] J.J.E. Moreau, M.W.C. Man, Coord. Chem. Rev. 178-180 (1998) 1073.
[25] R.A. Lal, L.M. Mukherjee, A.N. Siva, A. Pal, S. Adhikari, K.K. Narang, M.K. Singh, Polyhedron 12 (1993) 2351.
[26] A. Choplin, F. Quignard, Coord. Chem. Rev. 178-180 (1998) 1679.
[27] D.E. De Vos, M. Dams, B.F. Sels, P.A. Jacobs, Chem. Rev. 102 (2002) 3615.
[28] M. Salavati-Niasari, Chem. Lett. 34 (2005) 1444.
[29] M. Salavati-Niasari, Inorg. Chem. Commun. 8 (2005) 174.
[30] S.W. Wang, H. Everett, R.A.W. Haul, L. Moscou, R.A. Pierotti, J. Rouquerol, T. Siemieniewska, Pure Appl. Chem. 57 (1985) 603.
[31] A. Lineares-Solano, Textural characterization of porous carbons by physical adsorption of gases, in: J.L. Figueiredo, J.A. Moulijn (Eds.), Carbon and Coal Gasification, M. Nijhoff, M.A. Dordrecht, 1986, p. 137.
[32] W.J. Geary, Coord. Chem. Rev. 7 (1971) 81.
[33] L.M. Jackman, S. Sternhell, Application of Nuclear Magnetic Resonance Spectroscopy in Organic Chemistry, vol.10, 2nd ed., Pergamon Press, Amsterdam, 1978, chapter 3.
[34] B.N. Figgis, Nature 182 (1958) 1563.
[35] I. Bertini, G. Canti, R. Grassi, A. Scozzafava, Inorg. Chem. 19 (1980) 2198.
[36] N. Raman, Y.P. Raja, A. Kulandaisamy, Proc. Indian Acad. Sci. (Chem. Sci.) 113 (2001) 183.
[37] A.B. Lever, Inorganic Electronic Spectroscopy, 2nd ed., Elsevier, New York, 1968.
[38] M.A. Hitchman, Inorg. Chem. 16 (1977) 1985.
[39] M. Salavati-Niasari, Inorg. Chem. Commun. 7 (2004) 963.
[40] M. Salavati-Niasari, F. Davar, Inorg. Chem. Commun. 9 (2006) 304.
[41] M. Wang, C.J. Hao, Y.P. Wang, S.B. Li, J. Mol. Catal. 147 (1999) 173.
[42] C. Jin, W. Fan, Y. Jia, B. Fan, J. Maa, R. Li, J. Mol. Catal. A Chem. 249 (2006) 23.
[43] M. Salavati-Niasari, J. Mol. Catal. A Chem. 217 (2004) 87.
[44] M. Salavati-Niasari, J. Mol. Catal. A Chem. 229 (2005) 159.
[45] M.R. Maurya, S.J.J. Titinchi, S. Chand, J. Mol. Catal. A Chem. 214 (2004) 257.
[46] B.M. Choudary, M.L. Kantam, B. Bharathi, P. Sreekanth, F. Figueras, J. Mol. Catal. A Chem. 159 (2000) 417.
[47] I.F.J. Vankelecom, R.F. Parton, M.J.A. Casselman, J.B. Uytterhoeven, P.A. Jacobs, J. Catal. 163 (1996) 457.
[48] K.O. Xavier, J. Chacko, K.K.M. Yusuff, J. Mol. Catal. A Chem. 178 (2002) 275.